Water Science & Technology

Water Science & Technology Vol 00 No 0, 1 doi: 10.2166/wst.2026.237

Potential of mitigation strategies to compensate climate change impacts on the urban drainage network and pluvial flood hazard

Martina Hauser [a,*], Jaya Kelvin [b] and Manfred Kleidorfer [a]

[a] University of Innsbruck, Unit of Environmental Engineering, Technikerstraße 13, Innsbruck 6020, Austria
[b] Hydro & meteo GmbH, Breite Straße 6-8, Lübeck 23552, Germany
*Corresponding author. E-mail: martina.hauser@uibk.ac.at

MH, 0009-0006-7218-2490; JK, 0000-0001-7253-6857; MK, 0000-0002-4001-1711

ABSTRACT

Urban flooding is a growing global challenge, driven primarily by climate change and rapid urban development, which place increasing pressure on urban drainage networks. This study investigates the impacts of climate change and mitigation strategies in Innsbruck, Austria. Future periods are represented by design rainfall events scaled using climate change factors derived from bias-corrected convection-permitting simulations, while mitigation strategies are modelled by reducing the impervious connected area by 10, 20, and 30%. The results show climate change factors that indicate a strong intensification of short-duration, frequent rainfall and an increase by more than 31% in sewer surcharge and surface flooding under future conditions. Reducing the impervious connected area by 30% effectively counteracts the negative impacts of climate change in extreme events. However, the benefits of decoupling strategies are more pronounced for moderate precipitation events than for extreme ones and vary from <50 to >350 m^3/ha surcharge reduction between districts. The analysis highlights that a spatially heterogeneous strategy is more effective, as decoupling is more effective in districts with high hydraulic pressure. These findings demonstrate a clear potential of decoupling measures to mitigate climate change impacts on urban drainage, but underscore the need for strategic implementation to maximize effectiveness.

Key words: climate change, decoupling strategies, flood modelling, pluvial flooding, sewer surcharge, urban drainage network

HIGHLIGHTS

- Climate change intensifies pressure on the urban drainage network.
- Decoupling is more effective for moderate events than for extreme events.
- Reduction in surcharge volume per district area ranges from 50 to 350 m^3/ha.
- 30% reduction of impervious area reduces surcharge and flooding and offsets climate change impacts in extreme events.

GRAPHICAL ABSTRACT

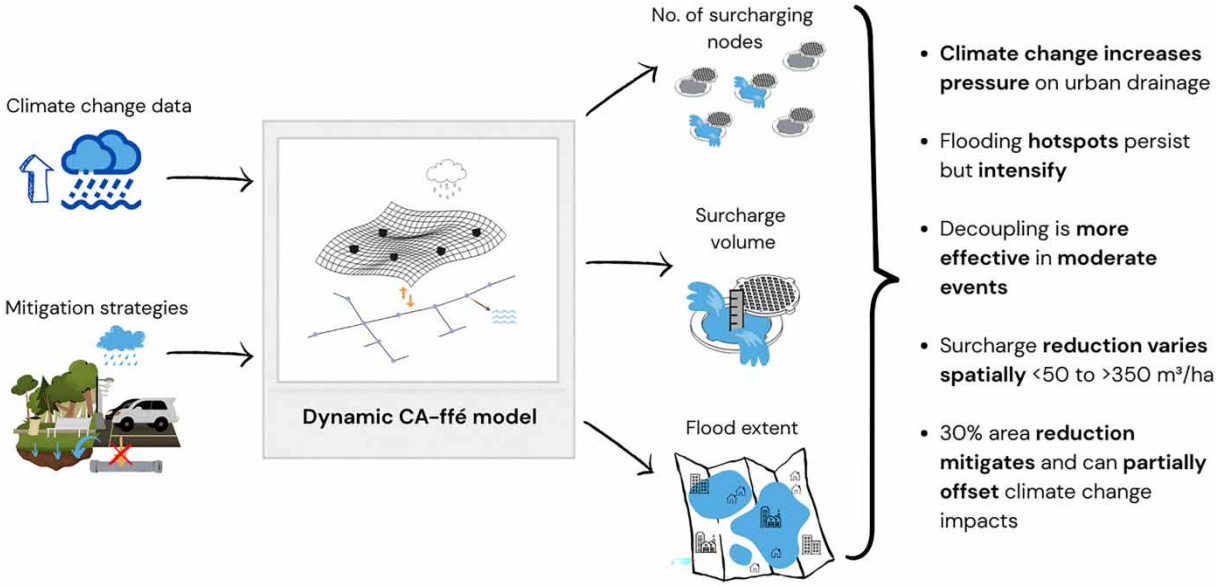

1. INTRODUCTION

Urban drainage systems, originally designed to collect, transport, and treat stormwater and wastewater runoff, face increasing challenges due to climate change and urban development. Further challenges, such as pipe and pump failures, blockages, sediment accumulation, and long-term asset deterioration, may also cause urban flooding (Funke *et al.* 2025) but are not considered in this study. Rising temperatures increased the atmosphere's water-holding capacity, resulting in more intense and frequent extreme precipitation events. The accelerating global trends of climate change and urban development amplify risks and expose vulnerabilities in urban infrastructure. The combined pressures lead to increased frequency and severity of extreme events and resulting urban pluvial flooding (Kundzewicz *et al.* 2017; Almazroui *et al.* 2021; Hosseinzadehtalaei *et al.* 2021).

Studies have shown increased overloading of sewer networks and surface flooding linked to more frequent extreme precipitation events (Wartalska *et al.* 2025). Former studies indicated that urban flood volume in the case study Hohhot, northern China, is projected to increase by 52% over 2020–2040 compared to the volume in 1971–2000 under the RCP8.5 scenario (Zhou *et al.* 2018). Nie *et al.* (2009) even mention that water volume from flooded manholes will increase 2–4 times the increase in precipitation in Veumdalen catchment in Fredrikstad, Norway. Long-term evaluation of precipitation records in Austria has shown that hourly heavy rainfall events have increased by approximately 15% over the last four decades (Haslinger *et al.* 2025), while average precipitation events exhibit strong seasonal and regional variability (APCC 2025). In parallel, urbanization expands impervious surfaces and leads to increased impervious areas, thereby shifting the urban water balance toward runoff-dominated regimes as infiltration is reduced, thereby increasing total stormwater volumes (Kim *et al.* 2025). The combined effects of urbanization and climate change pose a pressing challenge (Miller & Hutchins 2017). These pressures overwhelm drainage capacity and cause pluvial flooding (Kleidorfer *et al.* 2009, 2014). Strategic spatial planning plays a critical role in mitigating these impacts (Mikovits *et al.* 2017).

In response, cities are shifting from conventional grey infrastructure to blue-green infrastructure (BGI) that integrates ecological processes into urban design (de Rijke *et al.* 2025). Traditional networks prioritize rapid conveyance out of the city (Kim *et al.* 2016), but capacity expansion is costly, especially in dense urban areas, and can displace hydraulic load downstream (Arnbjerg-Nielsen *et al.* 2013). Therefore, decentralized BGI, such as green roofs, permeable pavements, bioretention cells, and vegetated swales, offers a sustainable, resilient and multifunctional alternative (Ariyarathna *et al.* 2023). By promoting infiltration, evapotranspiration, and temporary storage near the source, BGI reduces peak flows and volumes while delivering co-benefits for water and air quality, heat mitigation, biodiversity, and public health (Ariyarathna *et al.* 2023). A key hydrological strategy is the decoupling of impervious areas, routing runoff to adjacent pervious zones

or engineered BGI facilities for infiltration, treatment, or storage (Wang *et al.* 2019). The effectiveness of this decoupling approach has been proven by several studies, showing that implementing decoupling strategies is effective (Khadka *et al.* 2020; Sagar Kumar & Umamahesh 2025) and can reduce peak runoff by up to 12% in modelling and field surveys (Hwang *et al.* 2017).

Modelling tools are essential for analyzing the behavior of urban drainage systems and mitigation strategies. The Storm Water Management Model (SWMM) is widely used for rainfall-runoff processes and sewer hydraulics (Rossman 2015), but it cannot represent the spatial distribution of surface flooding (Abdelrahman *et al.* 2018). To simulate water depth and flood extent of surcharge volume on the surface, 2D models are required. Two-dimensional solvers of the shallow water equations provide detailed depths and extents but are computationally intensive for city-scale and multi-scenario studies. Cellular automata (CA) approaches offer a computationally efficient alternative by discretizing surfaces and routing water between neighboring cells based on elevation-driven transition rules (Ghimire *et al.* 2003). The parallelization of CA further enhances the simulation speed, providing the possibility for multiple simulation runs. Coupling SWMM with a CA-based surface model enables the representation of sewer-surface interaction at practical runtimes: runoff is generated in SWMM subcatchments, and surcharge can exit at nodes to the surface, also surface flows can re-enter the system through inlets when capacity is available. In this work, Dynamic CA-ffé (Gholami Korzani *et al.* 2026) is used as an addition to the SWMM model to simulate surcharge redistribution on the surface at high resolution with fast computation. This coupled, computationally efficient 1D/2D framework allows for testing multiple return periods and time horizons (past, near future, far future) and to compare mitigation strategies efficiently at city-scale.

For cities such as Innsbruck, characterized by a pronounced climate change signal, ongoing urban densification within constrained topography, and a combined sewer system, a detailed, site-specific analysis of sewer and surface flooding impacts is essential (Mikovits *et al.* 2017; Rosenzweig *et al.* 2018). The study aims to evaluate how climate change affects Innsbruck's sewer-system performance, such as surcharge volume and number of flooded nodes, as well as the resulting surface-flooding consequences across multiple time horizons (past, near future, far future), and to what extent BGI strategies can mitigate these consequences. Despite substantial work on climate and urbanization impacts, BGI benefits, and existing modelling tools, a clear gap remains: city-scale assessments using advanced approaches and explicit tests of whether the projected climate signal and system response differ between 1D sewer models and coupled 1D/2D representations of surface flooding. The novelty of the work lies in utilizing a fast, city-scale surface flood analysis that enables high-resolution mapping and expansive scenario exploration, thereby supporting strategic adaptation planning by a systematic comparison of climate change impacts and effectiveness of decoupling strategies in 1D (SWMM) versus coupled 1D/2D (Dynamic CA-ffé) representations. Thereby, the key advantage of Dynamic CA-ffé is the ability to give insights on flood extent and spatial patterns which cannot be derived from the 1D SWMM alone.

1.1. Case study

The city of Innsbruck in Austria serves as a case study for this study. As an alpine city in the European Alps, Innsbruck is facing amplified climate change combined with a growing city center. Therefore, Innsbruck is a case study that faces challenges similar to those faced by many other alpine cities worldwide. The European Alps are recognized as a hotspot for climate change as they respond more rapidly and intensely to global warming than lower-lying areas (Fuchs *et al.* 2025). Auer *et al.* (2007) showed that the average temperature in Austria has risen by approximately 2 °C since 1880, roughly double the global average. Climate projections for the Austrian Alps indicate a further intensification of this trend with a significant seasonal shift in precipitation (Laghari *et al.* 2012). Furthermore, they predict an increase in frequency and intensity of extreme precipitation events across all seasons (Gobiet *et al.* 2014). A 1 °C increase in temperature is projected to raise the precipitation intensity of short-term events by about 10% (APCC 2025), which is especially critical for the drainage network and pluvial flooding.

The urban form of the city is mainly shaped by the location in a narrow alpine valley and the river Inn. The inner city is already densely populated, and the city experiences a continuous pressure for urban growth and development as it is a major local economic and cultural center. This ongoing development leads to an increase in impervious area, which affects the stormwater runoff entering the drainage network. However, the city government also encourages a decoupling strategy, meaning that residents need to treat stormwater on site using decentralized systems, i.e., infiltrating on their own property. Based on the Austrian guideline (ÖWAV-RB45 2015), new properties, with a few exceptions, are not allowed to discharge stormwater to the public drainage network. This approach has already enabled several hectares of impervious area to be

disconnected from the sewer network, thereby making the system more sustainable. However, even if decoupling strategies using BGI are beneficial for mitigating sewer surcharge and surface flooding, they may increase groundwater recharge (Wu & Willems 2025), potentially causing basement seepage and embankment instability.

The urban drainage network in Innsbruck is mostly a combined sewer system. A combined sewer system is especially sensible during intense precipitation, as stormwater and wastewater are transported in a single pipe. The network of Innsbruck consists of approximately 258 km of pipe length and leads to the wastewater treatment plant (WWTP) in the eastern part of the city (IKB 2024).

The case study area covers approximately 51.33 km^2 and is divided into 173 districts (Figure 1).

2. METHODS

The coupled 1D/2D model Dynamic CA-ffé was used to evaluate different scenarios. The study focuses on assessing climate change impacts and the effects of mitigation strategies on pluvial flooding. Additionally, district-level decoupling scenarios were examined to identify the most vulnerable areas and those where mitigation would be most effective.

2.1. Climate change scenarios

Climate simulations were analyzed for three 30-year periods: 1971–2000 (past), 2031–2060 (near future), and 2071–2100 (far future). We used a convection-permitting simulation (CPS; COSMO-CLM) driven by the CMIP5 global model MIROC5 under the high-emission scenario RCP8.5 (Rybka *et al.* 2022). This dataset was selected because it provides hourly output at about 3 km resolution and continuous 30-year slices to support the analysis of short-duration precipitation extremes in complex Alpine terrain.

At the time this study was conducted, the simulations were available only under RCP8.5. This pathway was used as a stress-test of future pluvial flood hazard. Other emissions pathways could lead to different changes in precipitation extremes. This scenario dependence is not quantified here due to a lack of equivalent convection-permitting model output with comparable temporal coverage.

Model output was bias-corrected using observations from Innsbruck Airport (2000–2019) as the local reference. The bias-correction parameters were set up using the HoKliSim-De evaluation run, an ERA5-driven CPS simulation for the same period, and then applied consistently to the GCM-driven CPS time slices. Daily minimum and maximum temperatures were corrected using Quantile Delta Mapping (QDM) to align the simulated and observed distributions while preserving simulated changes across quantiles (Cannon *et al.* 2015). Hourly precipitation was corrected using a temperature-conditioned

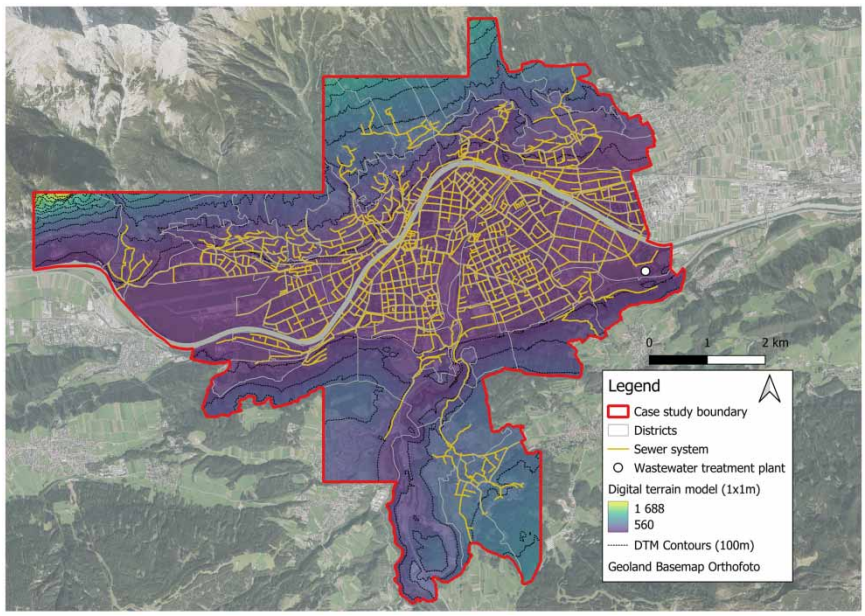

Figure 1 | Case study Innsbruck, including the drainage network, the wastewater treatment plant, the districts, and the digital terrain model.

quantile mapping approach to adjust intensity distributions while maintaining a physically consistent relationship between temperature and extreme rainfall. The temperature dependence of extreme hourly precipitation (99.9th percentile) before and after correction to check the physical consistency of extremes was also evaluated. Further diagnostic plots for the bias correction (temperature scatter plots, precipitation distribution checks, annual totals, and the temperature scaling of extreme precipitation) are provided in the Supplementary material, which accompanies this manuscript. The bias-corrected temperature indicates a mean end-of-century warming of 4.39 °C in Innsbruck (relative to 1971–2000) under RCP8.5, with a 5–95% interannual range of 2.93–6.66 °C based on annual means. This magnitude is consistent with the Second Austrian Assessment Report on Climate Change (AAR2), which reports Austria-wide late-century warming of around 4.9 °C under the highest warming level and highlights systematically stronger warming in western Austria and the Alpine region (APCC 2025). The spread reported in AAR2, particularly for summer temperature changes in the western region, reaches values of up to about 8 °C, indicating substantial interannual variability around the mean signal.

Precipitation changes were evaluated in terms of extremes rather than means. Annual maxima were extracted from the hourly bias-corrected precipitation for durations from 1 to 24 h and fitted with a Gumbel distribution using maximum likelihood estimation. Return levels were estimated for return periods of 1, 2, 3, 5, 10, 20, 25, 30, 50, 75, and 100 years. For each duration and return period, climate-change factors were calculated as the ratio of future to historical return levels. These factors were then used to scale the regional intensity–duration–frequency (IDF) curves from the Austrian hydrological portal (https://ehyd.gv.at/), ensuring consistency with national design standards, to generate future IDF relationships and to construct Euler Type II design-storm hyetographs for the hydraulic simulations. The Euler II design storm can be used for hydrodynamic modelling and stormwater drainage (Wartalska *et al.* 2020) and is recommended by the Austrian guideline (ÖWAV-RB 11 2009). Design storms are also advantageous for comparing the impact of climate-change signals across different return periods, as their temporal structure remains constant. In contrast, using observed rainfall events can complicate interpretation, since differences in event structure may introduce hidden effects. However, as design storms are based on standardized hyetograph shapes, they represent a simplified description of real rainfall events, and the choice of the design storm and the rainfall duration has a significant impact on the flood modelling results (Krvavica & Rubinić 2020). Critical pluvial floods are often associated with short, high-intensity bursts that should be captured by high-resolution rainfall data. In contrast, continuous 30-year simulations are computationally prohibitive at the city scale, especially with coupled 1D/2D approaches.

This study used one convection-permitting model chain and one emissions pathway (RCP8.5). The derived change factors are therefore conditional on this specific modelling chain and should be interpreted as a high-end stress test of drainage performance rather than as a probabilistic prediction of future change. We did not quantify sensitivity to other GCMs, CPS configurations, or alternative pathways (including CMIP6/SSP). In addition, while the change factors are derived from convection-permitting simulations, the hydraulic model is forced with IDF-scaled design storms. These represent duration and frequency statistics, but they do not represent event-to-event storm footprints, storm-cell placement, or sub-city spatial variability in rainfall.

2.2. Modelling approach

To analyze the effects of climate change and a decrease in impervious areas the Dynamic CA-ffé model was used. Dynamic Ca-ffé was originally developed by Jamali *et al.* (2019) and further developed by Gholami Korzani *et al.* (2026). Hauser *et al.* (2025) adapted the framework for bigger and alpine case studies by implementing the use of multiple rainfall data, land surface classification-based runoff coefficients, and the integration of buildings. The model combines a one-dimensional (1D) hydrodynamic sewer network model with a surface model based on cellular automata (CA). The 1D hydrodynamic model is a SWMM (Rossman 2015), which is used to simulate runoff and overflow behaviour in sewer networks. It is detailed and therefore more computationally intensive, but this allows for an also detailed analysis of individual sections or nodes. The simulation can be event-based or based on design rainfall. The 1D hydrodynamic model of Innsbruck includes more than 137,000 subcatchments, 6,400 nodes and 6,800 conduits and has been calibrated and validated by Herzog (2024) using water level and discharge measurements.

The CA surface model is based on a digital terrain model that includes buildings and runoff coefficients with a resolution of 1×1 m and elevations ranging from 560 up to 1,688 m.a.s.l. The software combines the 1D SWMM model with the CA-based surface model and thereby allows the water to flow on the surface, enter the sewer network, escape the network, and also to re-enter the system if sufficient capacity is available. It allows for different approaches to precipitation input, depending on

whether the rain is applied to the 1D SWMM model or as rain on grid in the CA surface model. In the approach used in this study, the rainfall is applied to the SWMM subcatchments, and the runoff simulation of SWMM is used to generate runoff that discharges to defined outlets such as sewer network nodes. When surcharge occurs, the volumes escaping the sewer system at specific nodes, as computed by SWMM, are transferred to the surface domain and redistributed using CA transition rules, as explained by Gholami Korzani *et al.* (2026). The CA model replaces the conventional surface runoff routing by explicitly simulating overland flow and flood inundation on a two-dimensional grid. The interaction between the sewer network and the surface is implemented through a soft, interval-based coupling, allowing water to leave the sewer system during surcharge conditions and to re-enter the network via inlets as surface water accumulates. The Dynamic CA-ffé model concept was validated by Gholami Korzani *et al.* (2026) for two Australian case studies by comparing the model results with 1D/2D hydrodynamic modelling results of another software. As validation of city-scale 2D models is a general issue, as there are hardly any measurements on the surface available, unfortunately, for the Innsbruck model, only simplified validation based on fire brigade operations was possible, as there is no existing city-scale 2D model for comparison and no measurement data of surface flooding available. As the flood volume originates from the sewer network, the main areas of interest are Innsbruck's flatter, urbanized valley floors. The results of the simulation focus on the flood areas on the surface, as well as the sewer network simulation, primarily in the urbanized areas of the case study.

The Dynamic CA-ffé model of the city of Innsbruck was used to analyze different scenarios. Based on the results of the 1D hydrodynamic simulation, the behavior of the network of the Innsbruck case study network was analyzed in terms of sewer surcharge volume and the number of surcharging nodes. The coupled 1D/2D model was then used to analyze how the surcharged volume propagates to surface flooding.

2.3. Scenarios of mitigation strategies

These scenarios examine the impact of mitigation strategies on the urban drainage system. Decentralized blue–green infrastructures (BGI), such as green roofs, permeable pavements, bioretention cells, and vegetated swales, promote infiltration, evapotranspiration, and local storage, thereby reducing runoff peaks and volumes while delivering co-benefits for water and air quality, heat mitigation, biodiversity, and public health (Ariyarathna *et al.* 2023). A key strategy is the disconnection of impervious areas, routing runoff to pervious surfaces or engineered BGI systems for infiltration, treatment, and storage (Wang *et al.* 2019).

To analyze these effects, a simplified approach was used to model the implementation of BGI and decentralized systems, whereby the impervious roof and street areas connected to the drainage system were reduced. Meaning that, all connected impervious street and roof areas in the SWMM model of the entire city of Innsbruck were reduced by rates of 10, 20 and 30%. This range was selected to demonstrate the impact of mitigation strategies at different levels of implementation. In consultation with the sewer network operator and based on previous investigations (Herzog 2024) of the connected areas, a decoupling rate of 10–30% can be considered realistic. This method provides a rough estimation of the general effects of surface decoupling strategies. This simplified method does not account for infiltration capacity and depression storage of BGI, which would potentially also impact the flood situation. In reality, certain areas are more sealed than others, and the potential for decoupling strategies varies based on settlement structure. In Innsbruck, for instance, the inner city is very densely populated and has a high proportion of sealed areas, whereas the surrounding areas are less densely populated and are also used for agriculture. Therefore, the analysis of decoupling strategies was also applied at the district level. Specifically, impervious street and roof areas within each district were reduced by up to 30%, and the resulting impacts on the citywide flooding situation were evaluated. This means that the uniform 30% reduction was first applied across the entire Innsbruck case study area, and then implemented individually in each of the 173 districts, meaning that decoupling strategies were applied for only one district per simulation run. This allows the identification of those districts where decoupling measures provide the greatest overall benefit at the city scale.

2.4. Evaluation methods

The results of the climate change analysis are presented as climate change factors, which are then multiplied by the design rainfall events. These events are then used as input data for the model, which analyzes the impact of climate change on the drainage network and surface flooding by evaluating changes in surcharge volume, the number of surcharging nodes (>10 m^3 surcharge), and the flooded area (>10 cm water depth). The threshold of 10 cm water depth refers to the maximum water depth and was set based on the Municipal agency NRW (2016) to account for flooding that could potentially endanger

buildings and people. To analyze the effects of mitigation strategies, a simplified approach involving a reduction in connected impervious area is used to demonstrate the impact on pluvial flooding. The results focus on reductions in terms of surcharge and flooding. Surcharge-related indicators, including surcharge volume and the number of surcharging nodes, are obtained from the SWMM model, whereas flooded areas and their spatial distribution are derived from Dynamic CA-ffé. Additionally, a district-based analysis evaluates districts in which decoupling measures are highly effective.

3. RESULTS AND DISCUSSION

3.1. Climate change projections

The convection-permitting simulations show a clear intensification of precipitation extremes over Innsbruck throughout the twenty-first century. The changes are consistent across all durations and return periods, but their magnitudes vary with event scale and rarity. For short-duration rainfall, the strongest relative increases are found for frequent events. Tables 1 and 2, respectively, present the climate change factors for the near and far future across durations and return periods. Over the 1-hour period, climate change factors reach 1.51 in the near future (2031–2060) and 1.54 in the far future (2071–2100) for the 1-year return period, corresponding to roughly a 50% increase relative to the historical baseline (1971–2000). The factors gradually decrease with rarity, reaching 1.26 and 1.16 for the 100-year return period. This pattern means that moderate but frequent convective rainfall becomes much more intense, while the rarest events still increase but less steeply in relative terms. For longer durations, the pattern changes. The 6-hour events show nearly constant near-future factors around 1.18, but far-future factors rise from 1.32 for short return periods to 1.43 for 100-year events. A similar signal is found for the 12-hour duration, increasing from roughly 1.30 to 1.40 in the far future, and for the 24-hour totals, which increase from 1.12–1.30 in the near future to 1.29–1.36 in the far future. This behavior indicates that frequent, short convective events are expected to intensify early in the century, while rarer, longer-lasting extremes strengthen later. Overall, the projected changes form an upward shift of the intensity-duration-frequency surface, implying stronger rainfall across scales.

The higher fractional increase for short, frequent events is consistent with the thermodynamic response of convective precipitation to warming. Warmer air holds more moisture, and convective updrafts can convert that moisture into precipitation at rates exceeding the 7% K^{-1} Clausius–Clapeyron scaling when latent heat release accelerates vertical motion. Observational and modelling evidence for such 'super-CC' behavior has been reported for hourly rainfall over Europe (Ban *et al.* 2015; Lenderink *et al.* 2021). In contrast, the most extreme or long-duration events are increasingly controlled by large-scale dynamics and moisture transport, which limit their relative intensification even as their absolute magnitude grows (Pfahl *et al.* 2017; Dallan *et al.* 2024).

Table 1 | Climate change factors under RCP8.5 for the near future period (2031–2060) by duration and return period

	Return period (years)										
Duration (min)	1	2	3	5	10	20	25	30	50	75	100
60 (1h)	1.51	1.30	1.29	1.28	1.28	1.27	1.27	1.27	1.27	1.27	1.26
120 (2h)	1.11	1.21	1.21	1.20	1.20	1.20	1.20	1.20	1.20	1.20	1.20
180 (3h)	1.09	1.18	1.19	1.20	1.21	1.22	1.22	1.22	1.23	1.23	1.23
240 (4h)	1.10	1.17	1.19	1.20	1.22	1.23	1.23	1.24	1.24	1.25	1.25
360 (6h)	1.19	1.18	1.18	1.18	1.18	1.18	1.18	1.18	1.18	1.18	1.18
540 (9h)	1.18	1.18	1.16	1.14	1.13	1.12	1.11	1.11	1.11	1.10	1.10
720 (12h)	1.21	1.19	1.17	1.16	1.14	1.13	1.13	1.13	1.12	1.12	1.11
1080 (18h)	1.26	1.22	1.20	1.18	1.16	1.15	1.15	1.15	1.14	1.13	1.13
1440 (24h)	1.30	1.22	1.20	1.18	1.16	1.14	1.14	1.14	1.13	1.12	1.12

Table 2 | Climate change factors under RCP8.5 for the far future period (2071–2100) by duration and return period

	Return period (years)										
Duration (min)	1	2	3	5	10	20	25	30	50	75	100
60 (1h)	1.54	1.41	1.35	1.30	1.25	1.21	1.20	1.20	1.18	1.17	1.16
120 (2h)	1.42	1.39	1.35	1.31	1.28	1.25	1.24	1.24	1.23	1.22	1.21
180 (3h)	1.39	1.34	1.32	1.30	1.28	1.26	1.26	1.26	1.25	1.24	1.24
240 (4h)	1.32	1.35	1.36	1.37	1.37	1.38	1.38	1.38	1.39	1.39	1.39
360 (6h)	1.32	1.33	1.35	1.37	1.39	1.40	1.41	1.41	1.42	1.42	1.43
540 (9h)	1.24	1.30	1.33	1.35	1.37	1.38	1.39	1.39	1.40	1.41	1.41
720 (12h)	1.30	1.30	1.32	1.34	1.36	1.37	1.38	1.38	1.39	1.39	1.40
1080 (18h)	1.25	1.30	1.32	1.33	1.34	1.35	1.35	1.35	1.35	1.36	1.36
1440 (24h)	1.36	1.29	1.30	1.31	1.32	1.32	1.32	1.32	1.33	1.33	1.33

The Innsbruck projections are in line with other Alpine studies based on kilometre-scale models. Ban *et al.* (2015) and Rybka *et al.* (2022) found that sub-daily extremes intensify more than daily totals despite little change in seasonal rainfall. Estermann *et al.* (2025) showed that kilometer-scale ensembles capture stronger elevation-dependent increases, particularly for short convective events. These projected increases are consistent with observations: Haslinger *et al.* (2025) reported a 15% increase in hourly heavy rainfall intensity across Austria over the last four decades.

To place the selected CPS dataset in a broader context, five additional convection-permitting simulations available from CORDEX-FPSCONV (10-year slices) (Supplementary material) were also compared. Across this small ensemble, warming is consistent, and the selected CPS lies within the ensemble spread for temperature change and upper precipitation quantiles, indicating it is not an outlier. This does not eliminate uncertainty in the magnitude of the derived change factors, but it supports using this CPS chain as a representative high-resolution case for Innsbruck.

The results presented here show that Innsbruck, like much of the Alpine region, is likely to face a future climate characterized by stronger and more concentrated rainfall. Frequent short events will become more intense first, while long-duration extremes will strengthen later in the century. Even if total rainfall does not increase substantially, more precipitation will fall in shorter bursts, increasing runoff potential and elevating flood risk in the city's dense and steep terrain.

The resulting climate change factors were used to construct the Euler Type II design storms (Figure 2) that force the hydraulic simulations.

3.2. Climate change impacts

Analyzing the impact of climate change projections on the urban drainage network and flood situation reveals an obvious upward trend in the risk of flooding in future periods. The number of surcharging nodes (>10 m^3 surcharge) and the surcharge volume increase in the near and far future, especially for higher return periods. The absolute increase from the past to the future is greater for higher return periods. For example, the $n = 50$ event increases by 4,516 m^3 in the near future and by a further 469 m^3 in the far future. In contrast, smaller return periods show a smaller absolute difference between the past and future periods. For $n = 5$, surcharge volume increases by 1,782 m^3 in the near future and by a further 1,001 m^3 in the far future. However, the relative increase, expressed as a percentage, for smaller events ($n = 5$) increases by 47% in the near future and 73% in the far future (compared to the past period), whereas higher events ($n = 50$) increase by only 41% in the near future and 45% in the far future. In general, higher return periods show a greater absolute difference between the past and near future, but only minor changes between the near and far future compared to smaller return periods. This means that extreme events lead to an even greater absolute increase in surcharge in the future.

A similar pattern is found for surface flooding (Figure 3). The flooded area (water depth >10 cm) increases further in the future and with higher return periods. Notably, higher return periods show a greater absolute increase from past to future

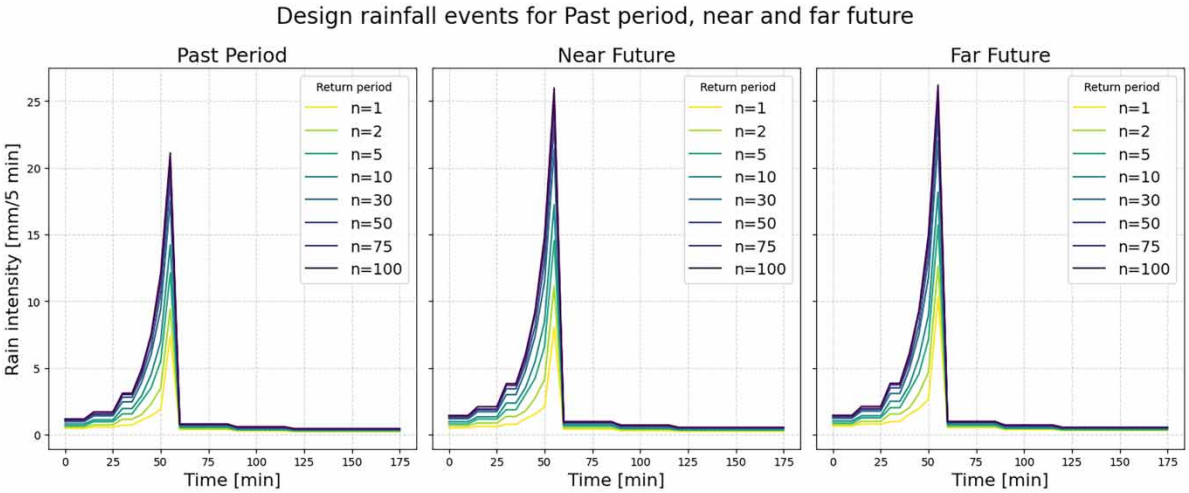

Figure 2 | Euler-II-Design-rainfall events for the past period, the near and the far future at different return periods.

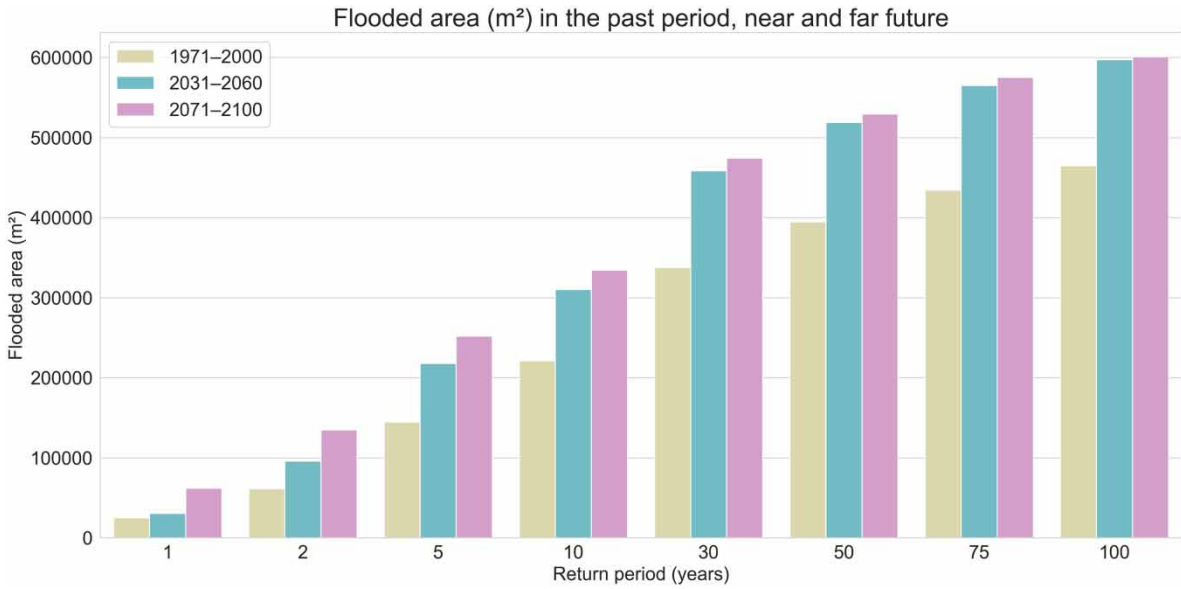

Figure 3 | Flooded area in the past period, near and far future for return periods 1, 2, 5, 10, 30, 50, 75, 100, each with a duration of 180 min.

periods, but a smaller increase between the two future periods. Smaller events ($n = 5$) increase by 51% in the near future and 75% in the far future (compared to the past period), and higher events ($n = 50$) by 31% in the near future and 34% in the far future. Although there is a logical connection between the two models, as the surcharge volume is spread by this modelling approach, the flooded area also depends on the elevation model. This means that the impacts of climate change cannot be transferred exactly from a change in sewer surcharge to a change in flooded area.

When analyzing the top 10 surcharging nodes (Figure 4), the top 10 nodes were very similar, but not the same, for all return periods and for all three time periods. Starting from return period $n = 2$, the node with the highest surcharge volume is RV02 (long name: MU03010_RV02). This node is located in the middle of the sewer network and serves as a starting point with a relatively shallow shaft. A map showing the location of the top flooded nodes is provided in the Supplementary material. Only in the return period $n = 1$, there is no flooding for this node in the past period and the near future. Generally, only a few new nodes are additionally flooded, and most nodes that are flooded in the past period are also flooded in future periods, with an increase in surcharge volume per node. This means that nodes which are problematic in the past are even more problematic

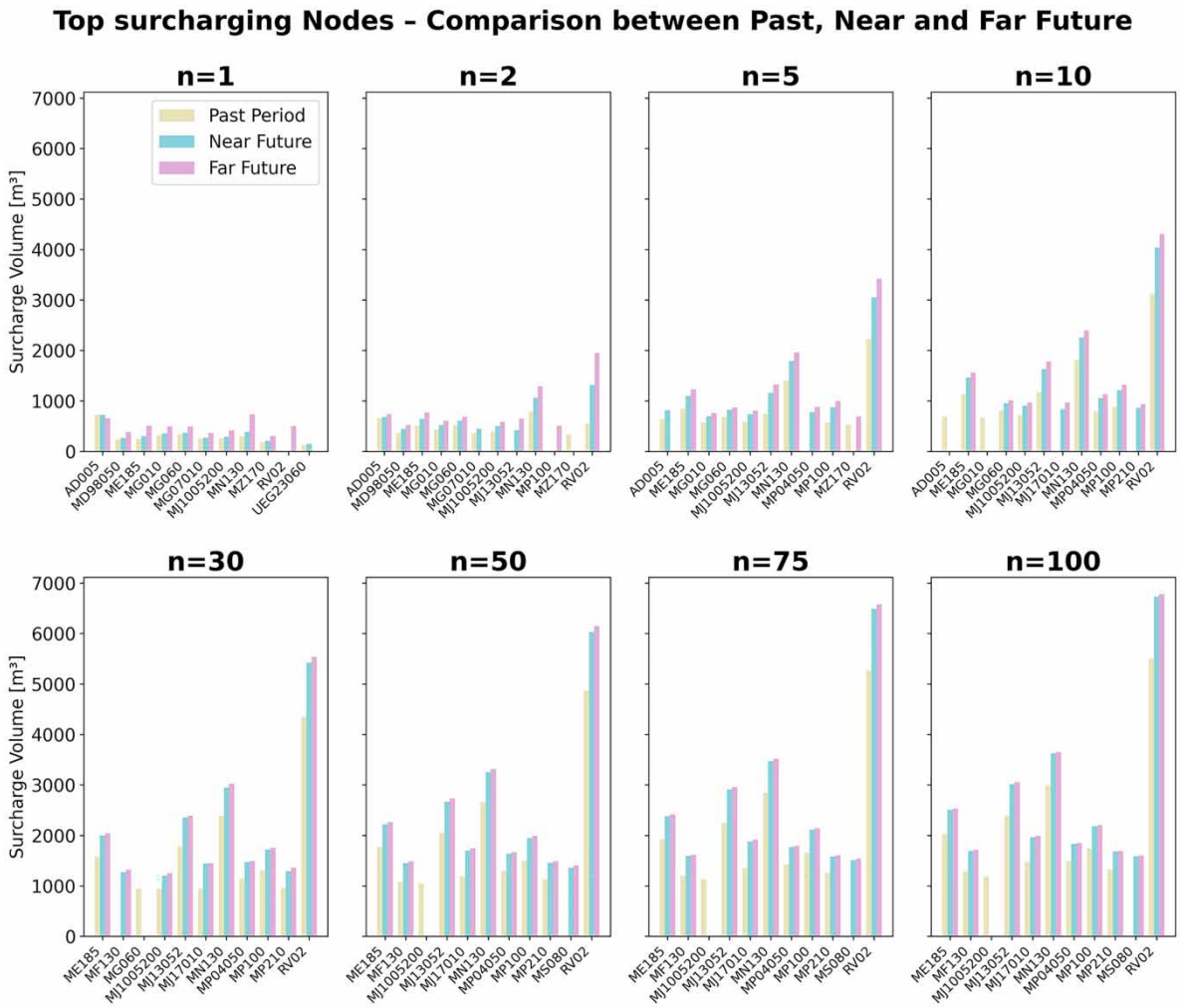

Figure 4 | Comparison of the top 10 surcharging nodes for return periods $n = 1$, 2, 5, 10, 30, 50, 75, 100 and 180 minutes duration for the past period, near, and far future.

in future periods. Conversely, certain nodes only surcharge in one period, not the other two. This means that changes in precipitation intensity do not affect the drainage network uniformly. Instead, they can alter the internal load distribution, causing surcharging to shift from previously critical nodes to other parts of the system. As a result, some nodes are relieved while new flooded nodes emerge. This non-linear and spatially heterogeneous response demonstrates that the impacts of increasing rainfall intensity cannot be inferred from local precipitation observations alone, but require detailed hydraulic modelling to identify where stresses will occur under changing conditions. Consequently, different rainfall temporal structures could modify local flooding patterns, although the identified hotspots and relative sensitivities are primarily controlled by network hydraulics and surface topography.

To analyze the changes in the flooded area, it was also necessary to identify whether hotspots change in future periods. Figure 5 shows the change in flooded area between the past period and the near future, and between the near future and the far future. Analyzing the change in flooded area (water depth >10 cm) between different time periods reveals that, between the past period and the near future, 39.0 hectares are flooded in the past period and are also flooded in the near future. A further 12.8 hectares are additionally flooded in the near future, while 0.47 hectares flooded in the past period are not flooded due to the characteristics of the drainage network and the elevation model. A similar situation appears when analyzing the change between the near and far future: 50.4 hectares are flooded in the near and far future, 2.6 hectares are additionally flooded in the far future, and 1.5 hectares flooded in the near future are not flooded in the far future. This indicates that 75% of the flooded area in the near future is also flooded in the past period, and 95% of the flooded area in

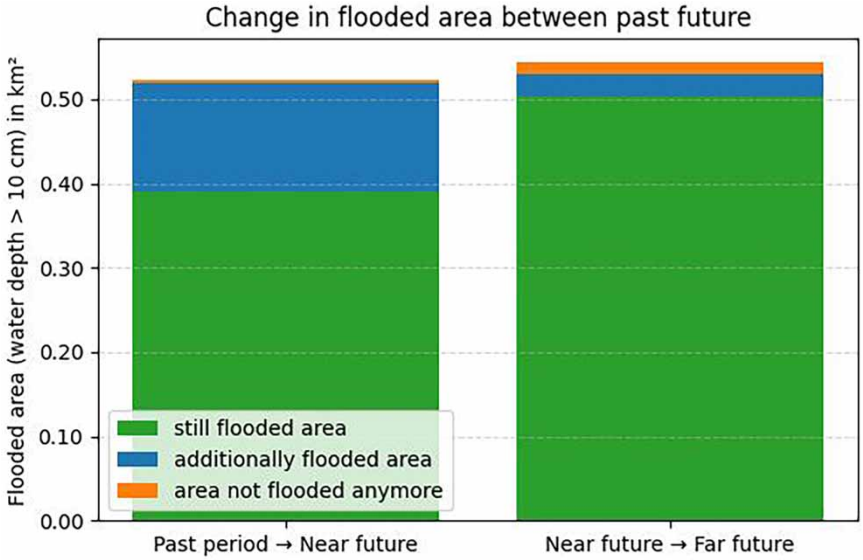

Figure 5 | Change in flooded area (in km^2, water depth >10 cm) between the past period and the near future, and the near and far future.

the far future is also flooded in the near future. Additionally, the flooded area increases by 31% from the past period to the near future, and by a further 2% from the near future to the far future. This indicates that the flooded area generally increases in the future, but cells that are flooded in previous periods tend to remain flooded in the future periods as well. This means that most hotspots will remain, but intensify in the future.

Visualization of flooded areas (>10 cm) in the past and future periods highlights that locations flooded in the past period tend to be more at risk in the future. However, the results for the flooded area depend heavily on the chosen threshold of 10 cm and the elevation model, as most of the flooded area has a water depth less than 25 cm. If water accumulates in depressions of the terrain model, there will be almost no change in the flooded area, even if there is more surcharging from the node. Conversely, if the terrain is very flat, even small increases in surcharge volume can have a significant impact on the flooded area. Figure 6 shows the flooded area (water depth >10 cm, $n = 50$) for the past period in pink and the far future in green underneath. Additionally, the increase (yellow) and decrease (red) in the area of flooding hotspots are highlighted by circles. The larger the circle, the greater the increase or decrease in flooded area from the corresponding hotspot (connected flooded cells in this area). Once again, it transpires that most hotspots that were flooded in the past period will also be flooded in the future, but to a greater extent.

A comparison of the two target values shows increased surcharge volume (derived from SWMM) and flooded area (derived from Dynamic CA-ffé) compared to the 1971–2000 reference period. Figure 7 compares the three target values for return periods of five and 50 years. For moderate events (a return period of five years, $n = 5$), the target values show an increase of 35% in number of flooded nodes, 47% in surcharge volume and 51% in flooded area for the period 2031–2060, and 81% in number of flooded nodes, 73% in surcharge volume and 74% in flooded area for the period 2071–2100. By contrast, the increase for extreme events (return period of 50 years, $n = 50$) is lower, at 37% in number of flooded nodes, 41% for surcharge volume and 31% for flooded area for the period 2031–2060, and 40% in number of flooded nodes, 45% for surcharge volume and 34% for flooded area for the period 2071–2100. This means that moderate events are projected to intensify the target values more strongly than extreme events. Nevertheless, all events will lead to a significant rise in surcharge and flooding by the end of the century. The small differences between the three values indicate a strong relationship between surcharge and flooding behaviour.

3.3. Mitigation strategy scenarios

The representation of mitigation strategies through a reduction in impervious area is a simplified approach to analyzing the effect of BGI and decentralized systems. Figure 8 illustrates the impact of changes in impervious surface area on surcharge volume and the number of nodes experiencing surcharging (>10 m^3 surcharge) based on moderate (return period five years)

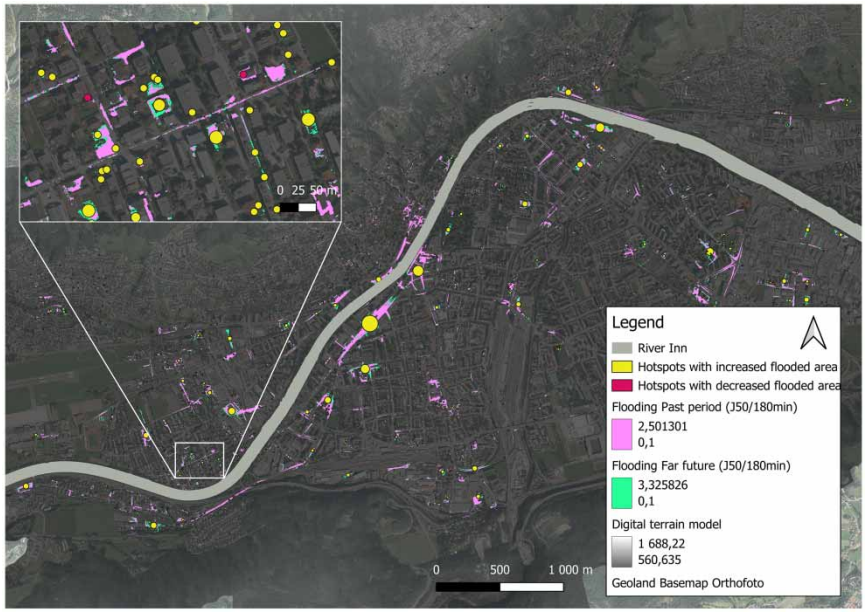

Figure 6 | Visualization of flooded area ($n = 50$) for the past period (pink) and far future (green), highlighting increase (yellow) and decrease (red) of flooded area in size-indicating circles.

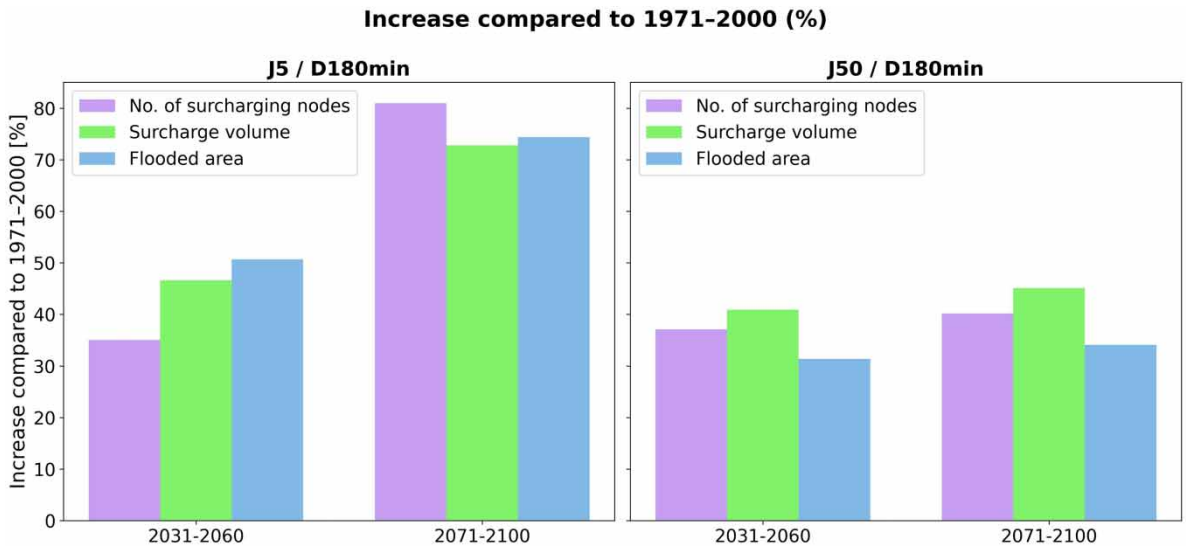

Figure 7 | Surcharge volume and flooded area for the near and far future in comparison to the reference period 1971–2000 (return periods five and 50 years, 180 min).

and extreme (return period 50 years) design events. Reducing impervious area by 10, 20, or 30% reduces both surcharge volume and the number of flooded nodes. This finding aligns with previous studies that demonstrated the effectiveness of BGI and mitigation strategies to reduce pluvial water discharge (Hussain *et al.* 2021; El Baida *et al.* 2025) and with the experience of the sewer operator who reported positive effects based on the decoupling strategies in the past years. The greater the reduction percentage, the greater the decrease in both target values. A 30% decrease lowers the surcharge volume by approximately 40–46% ($n = 5$) and 33 to 36% ($n = 50$) compared to the baseline. Similarly, a 30% reduction lowers the number of surcharging nodes by 28 to 33% ($n = 5$) and 19–24% ($n = 50$). This means that surface decoupling strategies are relatively more effective for moderate events ($n = 5$) than for extreme events ($n = 50$). However, the increase for future periods is

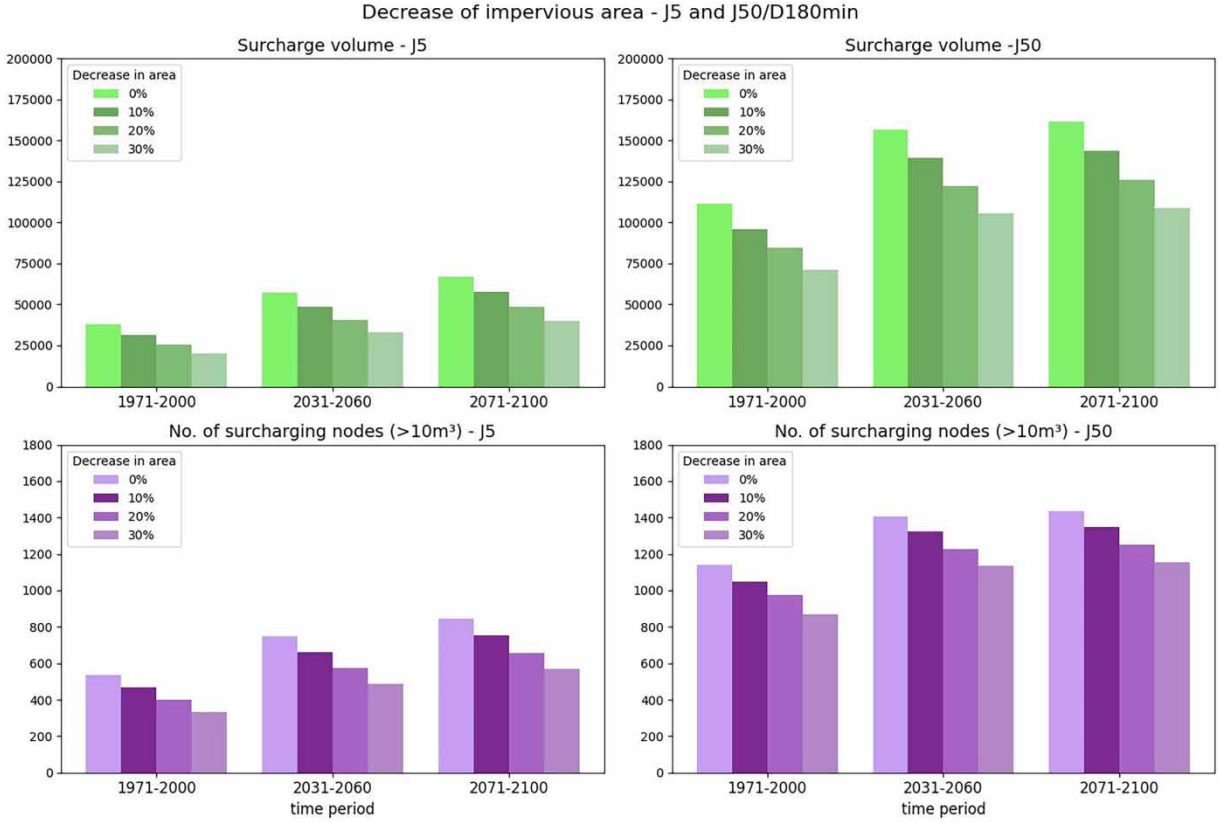

Figure 8 | Impact of 10, 20, and 30% decrease of impervious area on surcharge volume and number of flooded nodes for return periods of five and 50 years (duration 180 min) for the past period, the near and far future.

still notable, proving that climate change will intensify surcharging and flooding, and will partly offset the effects of surface decoupling measures.

A similar situation occurs when analyzing the flooded area. The flooded area decreases as impervious area decreases. This is consistent with Moon *et al.* (2024), who demonstrated a reduction in flooded area and flood volume by integrating mitigation strategies. A 30% reduction in the connected impervious area leads to a 31.3% ($n = 5$) and 16.1% ($n = 50$) total reduction in flood area in the period 1971–2000, a 27.8% ($n = 5$) and 12.9% ($n = 50$) reduction in the period 2031–2060, and a 23.5% ($n = 5$) and 13.9% ($n = 50$) reduction in the period 2071–2100. Analyzing across return periods shows that decoupling strategies reduce total flooded area more effectively for moderate events than for extreme events. This result is in line with many previous studies, such as Liu *et al.* (2014), Eckart *et al.* (2017), Huang *et al.* (2020) and Mugume *et al.* (2024). This will become even more important in the future, as the number of extreme pluvial flood events is set to increase (Kundzewicz *et al.* 2017; Almazroui *et al.* 2021; Hosseinzadehtalaei *et al.* 2021).

Figure 9 compares the reduction in all three target values for a 30% decrease in impervious area for moderate ($n = 5$) and extreme ($n = 50$) events. This comparison also allows one to identify differences between the 1D SWMM model and the coupled Dynamic CA-ffé model. The figure shows that decoupling has a similar impact on flooded area (derived from Dynamic CA-ffé), surcharge volume, and the number of surcharging nodes (both derived from SWMM). However, for extreme events ($n = 50$), the reduction in flooded area is smaller than the reduction in the other two indicators. This indicates that decoupling 30% of the impervious area leads to fewer surcharging nodes and surcharge volume, but especially in extreme events, flooding hotspots mainly remain, with decreased water depth, resulting in less overall reduction in flooded area. The impact on all target values is smaller for extreme events ($n = 50$) than for moderate events ($n = 5$). This indicates that decoupling strategies are most effective at reducing surcharge during moderate events. It should be noted that BGI eventually fails to infiltrate or store stormwater any further, leading to increased runoff. This effect is not explicitly represented in this study and would likely reduce the effectiveness of decoupling strategies, especially during extreme events.

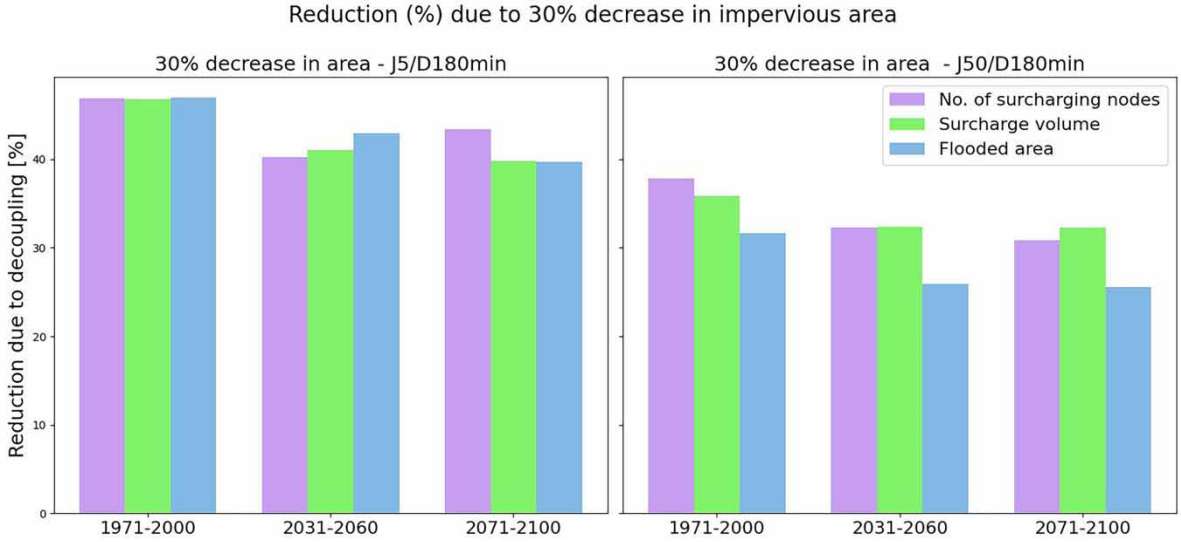

Figure 9 | Reduction (%) of the number of surcharging nodes, surcharge volume, and flooded area at 30% decrease in area for return periods five and 50 years (duration 180 min) for the past period, near, and far future.

Overall, a 30% reduction in impervious area during moderate events ($n = 5$) results in a flooded area of 124,293 m^2 in the near future and 152,110 m^2 in the far future. For comparison, the original flooded area without any mitigation strategies is 144,544 m^2, which is smaller than the far future scenario even when surface decoupling measures are applied. In extreme events ($n = 50$), implementing the 30% impervious area reduction leads to a flooded area of 384,143 m^2 in the near future and 393,983 m^2 in the far future. The original flooded area in this case is 394,893 m^2, which is higher than the future scenarios with mitigation. These results indicate that, with a 30% reduction in impervious area, the effects of climate change can be partially compensated, as for extreme events ($n = 50$), both future decoupling scenarios result in less flooded area, and for moderate events ($n = 5$), at least the near future decoupling scenario results in reduced flooded areas. This is also in line with former studies that revealed that nature-based solutions (NbS) can develop the adaptive capacity to offset some climate change impacts (Huang *et al.* 2020).

3.3.1. District analysis

To identify the districts that are most responsive to mitigation strategies, a 30% reduction in impervious area was applied to each district individually. Accordingly, 30% of impervious areas were decoupled in each of the 173 districts. This results in different absolute values for each district, as impervious areas vary between districts. In Innsbruck, for example, District 41 (in dark green, Figure 10) has the largest decoupled area because it has the greatest amount of impervious area. In general, inner-city districts are more sealed and therefore have more impervious areas. The surrounding districts have smaller impervious areas but are generally larger.

The quantitative and spatial effects of each reduction on the citywide flood situation were analyzed. Figure 10 shows the spatial variability of the hydraulic response to a 30% reduction in impervious surfaces across all districts. The analysis revealed significant differences between the various districts. There is significant heterogeneity across the entire city. Some districts in the west (e.g., 361) and the inner city districts experience high reduction rates, whereas districts in the south and east experience lower rates. The reduction in surcharge volume, normalized by the decoupled area per district, ranges from less than 50 m^3/ha to more than 350 m^3/ha. However, comparison with decoupled area reveals no direct correlation between area reduction and surcharge reduction per hectare. Districts with a high amount of decoupled area do not necessarily experience a high reduction in flooded area. This indicates that the effectiveness of decoupling strategies depends not only on the amount of decoupled area, but also on drainage system characteristics and district location. Districts with a high hydraulic load or lower system capacity tend to experience greater effects from such mitigation strategies than districts with lower surcharge risk or higher system capacity. Central districts also exhibit significant variations due to complex network interconnections and diverse connection conditions. This indicates that the effectiveness of surface decoupling

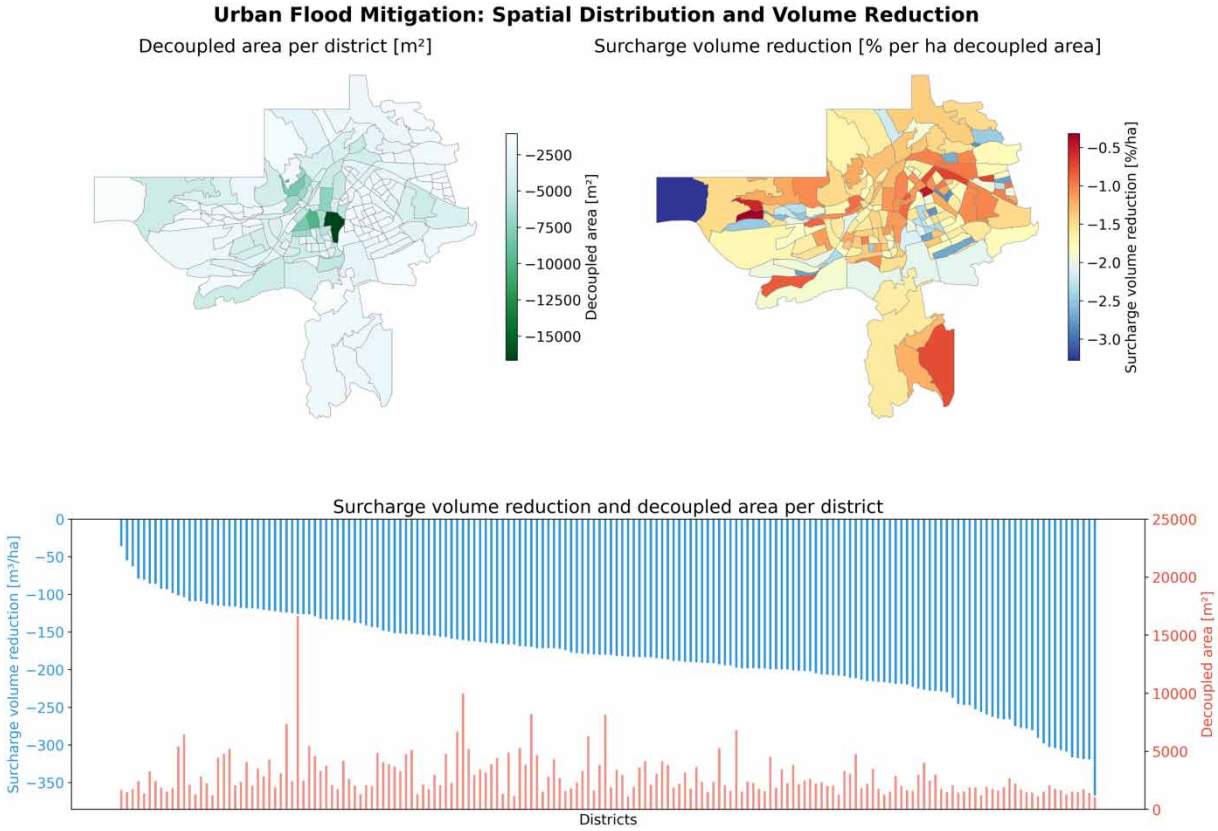

Figure 10 | Decoupled area per district with 30% decrease in impervious area, and a spatial graph and a bar plot of the reduction in surcharge volume per ha at 30% decoupling per district compared to decoupled area (m^2). Figures including district label numbering are provided in the Supplementary material.

measures depends on network characteristics such as topography and sewer capacity, meaning that the impact on the surcharge behavior across the city is not trivial and depends on the location of the district and the drainage network. Furthermore, decoupling in one district may also affect neighboring and especially downstream districts. Therefore, while the overall effect of 30% decoupling is positive, its impact is not uniformly distributed. This suggests that implementing such mitigation strategies in certain districts could be more beneficial, leading to greater improvement in the overall surcharge and flood situation than a uniform application would achieve. It has to be considered that the real potential of maximum decoupled area is different in each district and depends also on various factors such as topography or available space, as inner-city districts are already very sealed, whereas outer districts are more rural and provide much more pervious areas, not connected to the drainage network and therefore not apparent in the model analysis.

Figure 10 demonstrates high spatial variability across the city. Therefore, it is essential to prioritize districts with the highest reduction rates per decoupled area. A homogeneous decoupling strategy does not necessarily result in the best hydraulic improvement, as the reduction depends on the characteristics of the network and the digital terrain model. Liang *et al.* (2020) also mentioned that the efficiency of Low Impact Development (LID) controls can be improved by changing the spatial distribution of the LID controls to reduce the connected impervious area, and Ferreira *et al.* (2022) reported that NBS performance in flood protection is strongly linked to spatial allocations.

4. CONCLUSIONS

This study shows that climate change is expected to substantially intensify short- and long-duration precipitation extremes in Innsbruck. The strongest increases occur for short, frequent events, while rare, long-lasting extremes continue to strengthen toward the end of the century. As a result, future rainfall is projected to become more temporally concentrated and more

effective at generating runoff, even if total precipitation changes only slightly. These projected shifts in rainfall characteristics provide the physical basis for the higher hydraulic loads found in the drainage simulations.

The hydrodynamic analysis revealed an obvious upward trend for the near and far future. All three target values (surcharge volume, number of surcharging nodes (>10 m^3 surcharge), and flooded area (>10 cm water depth)) showed a clear increase, indicating additional pressure on the drainage network. Surcharge volume and flooded area increased by more than 31% under future conditions in the analyzed scenarios. The spatial distribution of flooded areas on the surface showed that future hotspots mostly remain where they were in the past, and they tend to intensify. The flooded area and surcharge volume increase, while nodes that are already critical tend to remain critical, but experience higher surcharge volumes. Analyzing the top surcharging nodes also supports this conclusion. These findings align with prior work reporting increased sewer overloading and surface flooding under intensified short-duration rainfall (e.g., Haslinger *et al.* 2025; Wartalska *et al.* 2025). The coupled 1D/2D framework extends this literature by providing fast, high-resolution, city-scale surface flood mapping, enabling broad scenario exploration and revealing consequence patterns that a 1D-only perspective would partially miss.

Decentralized BGI, especially impervious area disconnection, reduces all target metrics, with stronger percentage gains for moderate events than for the most extreme ones due to infiltration and storage limits at high intensities, consistent with earlier findings (e.g., Hwang *et al.* 2017; Khadka *et al.* 2020; Ariyarathna *et al.* 2023). This study neglects the fact that BGI fails to further infiltrate or store stormwater at a certain point, which would lead to a less positive impact in extreme events. Nevertheless, a general decrease in all three target values was notable. Comparing the three different target values revealed that for extreme events ($n = 50$), decoupling exerts greater influence on surcharge volume and the number of surcharging nodes than on total flooded area. Nevertheless, reduced surcharge lowers water depths in inundated zones, yielding meaningful but comparatively smaller reductions in flooded extent. Notably, 30% decoupling counteracts climate-driven increases in the near-future scenarios for both moderate ($n = 5$) and extreme ($n = 50$) events, echoing the direction of benefits reported in prior urban case studies (Huang *et al.* 2020), while adding city-wide, high-resolution surface consequence mapping as a novel element.

A key addition in this work is a district-level perspective to identify the most effective districts for decoupling strategies. The effectiveness and implementability of impervious surface disconnection depend on available space, topography, soil/infiltration capacity, groundwater, and existing utilities. This analysis reveals significant heterogeneity, indicating that the effectiveness of reducing surcharge volume per decoupled area depends heavily on the drainage network's characteristics and surface elevations. However, identification is highly specific to each case as it is based on the characteristics of the local drainage network, such as topography, roughness, losses, and interconnections.

Overall, pressure on Innsbruck's urban drainage networks will increase in future climate change scenarios, but mitigation strategies such as BGI, which reduce connected impervious areas, can meaningfully mitigate consequences if deployed strategically. The combination of climate-adjusted design storms and a fast, coupled 1D/2D workflow enables robust, city-scale exploration of futures and interventions, supports comparison with prior findings, and links consequence reductions to district-level feasibility to guide practical adaptation planning, even if estimation of sewer system performance is based on standardized design hyetographs.

Future work could therefore focus on complementing the present design-storm-based approach with simulations using real rainfall events and selected event series out of climate change projections to further assess the robustness of the findings under more realistic temporal rainfall structures.

ACKNOWLEDGEMENTS

The authors would like to thank Innsbrucker Kommunalbetriebe (IKB) for providing the necessary data on Innsbruck's sewer network and Antonia Herzog for providing the calibrated SWMM model as part of her master thesis.

AUTHOR CONTRIBUTIONS

M.H.: Conceptualization, Methodology, Software, Validation, Formal analysis, Investigation, Resources, Data Curation, Writing – Original Draft, Writing – Review and Editing, Visualization, Project administration, Funding acquisition. J.K.: Data Curation, Validation, Writing – Original Draft, Writing – Review and Editing. M.K.: Conceptualization, Resources, Writing – Review and Editing, Supervision, Project administration, Funding acquisition.

FUNDING

This work is funded by IKB Research Funding (project title: 'futuremode(l): Conceptual and Hydrodynamic Modelling of Innsbruck's Sewer System under Future Climate Change Conditions') from January 2024 to August 2025, and forms part of the BlueGreenCities project (project number KR21KB0K00001), which is funded by the Austrian Climate and Energy Fund from October 2022 to September 2025. The simulation results were generated using the LEO HPC infrastructure at the University of Innsbruck.

DATA AVAILABILITY STATEMENT

Data cannot be made publicly available; readers should contact the corresponding author for details.

CONFLICT OF INTEREST

The authors declare there is no conflict.

REFERENCES

Abdelrahman, Y. T., Moustafa, A. M. E. & Elfawy, M. (2018) Simulating flood urban drainage networks through 1D/2D model analysis, *Journal of Water Management Modeling*, **26**, C454. https://doi.org/10.14796/JWMM.C454.

Almazroui, M., Saeed, F., Saeed, S., Ismail, M., Ehsan, M. A., Islam, M. N., Abid, M. A., O'Brien, E., Kamil, S., Rashid, I. U. & Nadeem, I. (2021) Projected changes in climate extremes using CMIP6 simulations over SREX regions, *Earth Syst Environ*, **5**, 481–497. https://doi.org/10.1007/s41748-021-00250-5.

APCC (2025) *Second Austrian Assessment Report on Climate Change (AAR2)*, Huppmann, D., Keiler, M., Riahi, K. & Rieder, H. (eds.). Vienna: Austrian Academy of Sciences Press.

Ariyarathna, I. S., Abeyrathna, W. P., Jamei, E. & Chau, H.-W. (2023) A review of the application of blue–green infrastructure (BGI) as an effective urban flood mitigation strategy for livable and healthy cities in Australia, *Architecture*, **3**, 461–476. https://doi.org/10.3390/architecture3030025.

Arnbjerg-Nielsen, K., Willems, P., Olsson, J., Beecham, S., Pathirana, A., Bülow Gregersen, I., Madsen, H. & Nguyen, V.-T.-V. (2013) Impacts of climate change on rainfall extremes and urban drainage systems, *Water Science and Technology : A Journal of the International Association on Water Pollution Research*, **68**, 16–28. https://doi.org/10.2166/wst.2013.251.

Auer, I., Böhm, R., Jurkovic, A., Lipa, W., Orlik, A., Potzmann, R., Schöner, W., Ungersböck, M., Matulla, C., Briffa, K., Jones, P., Efthymiadis, D., Brunetti, M., Nanni, T., Maugeri, M., Mercalli, L., Mestre, O., Moisselin, J., Begert, M., Müller-Westermeier, G., Kveton, V., Bochnicek, O., Stastny, P., Lapin, M., Szalai, S., Szentimrey, T., Cegnar, T., Dolinar, M., Gajic-Capka, M., Zaninovic, K., Majstorovic, Z. & Nieplova, E. (2007) HISTALP – historical instrumental climatological surface time series of the Greater Alpine Region, *International Journal of Climatology*, **27**, 17–46. https://doi.org/10.1002/joc.1377.

Ban, N., Schmidli, J. & Schär, C. (2015) Heavy precipitation in a changing climate: does short-term summer precipitation increase faster?, *Geophysical Research Letters*, **42**, 1165–1172. https://doi.org/10.1002/2014GL062588.

Cannon, A., Sobie, S. & Murdock, T. (2015) Bias correction of GCM precipitation by quantile mapping: how well Do methods preserve changes in quantiles and extremes?, *Journal of Climate*, **28**, 150722131126009. https://doi.org/10.1175/JCLI-D-14-00754.1.

Dallan, E., Marra, F., Fosser, G., Marani, M. & Borga, M. (2024) Dynamical factors heavily modulate the future increase of sub-daily extreme precipitation in the alpine-mediterranean region, *Earth's Future*, **12**, e2024EF005185. https://doi.org/10.1029/2024EF005185.

de Rijke, C. A., Lim, N. J., Iqbal, A., Brandt, S. A. & Sahlin, E. A. U. (2025) A systematic review of blue-green infrastructure's role and relevance in the mitigation and management of climate-induced hazards in x-minute cities, *Planning Practice & Research*, **0**, 1–29. https://doi.org/10.1080/02697459.2025.2516529.

Eckart, K., McPhee, Z. & Bolisetti, T. (2017) Performance and implementation of low impact development – a review, *Science of The Total Environment*, **607–608**, 413–432. https://doi.org/10.1016/j.scitotenv.2017.06.254.

El Baida, M., Chourak, M. & Boushaba, F. (2025) Flood mitigation and water resource preservation: hydrodynamic and SWMM simulations of nature-based solutions under climate change, *Water Resources Management*, **39**, 1149–1176. https://doi.org/10.1007/s11269-024-04015-3.

Estermann, R., Rajczak, J., Velasquez, P., Lorenz, R. & Schär, C. (2025) Projections of heavy precipitation characteristics over the greater alpine region using a kilometer–scale climate model ensemble, *Journal of Geophysical Research: Atmospheres*, **130**, e2024JD040901. https://doi.org/10.1029/2024JD040901.

Ferreira, C. S. S., Potočki, K., Kapović-Solomun, M., Kalantari, Z., (2022) Nature-Based Solutions for Flood Mitigation and Resilience in Urban Areas. In: Ferreira, C. S. S., Kalantari, Z., Hartmann, T. & Pereira, P. (eds.) *Nature-Based Solutions for Flood Mitigation: Environmental and Socio-Economic Aspects*, Cham: Springer International Publishing, pp. 59–78. https://doi.org/10.1007/698_2021_758.

Fuchs, S., Schöner, W., Steiger, R., (2025) Chapter 7. The Austrian Alps as multi-dimensional focal area. In: Huppmann, D., Keiler, M., Riahi, K. & Rieder, H. (eds) *Second Austrian Assessment Report on Climate Change (AAR2) of the Austrian Panel on Climate Change (APCC)*, Vienna, Austria: Austrian Academy of Sciences Press. https://doi.org/10.1553/aar2-ch7.

Funke, F., Reinstaller, S. & Kleidorfer, M. (2025) Impact of urban drainage system malfunctions on pluvial flooding – peri-urban study site in Austria, *Journal of Hydrology: Regional Studies*, **60**, 102592. https://doi.org/10.1016/j.ejrh.2025.102592.

Ghimire, B., Chen, A., Guidolin, M., Keedwell, E., Djordjević, S. & Savic, D. (2003) Formulation of a fast 2D urban pluvial flood model using a cellular automata approach, *Journal of Hydroinformatics*, **15**, 676–686. https://doi.org/10.2166/hydro.2012.245.

Gholami Korzani, M., Chaudhary, A., Jamali, B. & Deletic, A. (2026) Dynamic CA-ffé: a hybrid 1D/2D fast flood evaluation model for urban flash floods, *Journal of Hydrology*, **665**, 134762. https://doi.org/10.1016/j.jhydrol.2025.134762.

Gobiet, A., Kotlarski, S., Beniston, M., Heinrich, G., Rajczak, J. & Stoffel, M. (2014) 21st century climate change in the European Alps – A review, *Science of The Total Environment*, **493**, 1138–1151. https://doi.org/10.1016/j.scitotenv.2013.07.050.

Haslinger, K., Breinl, K., Pavlin, L., Pistotnik, G., Bertola, M., Olefs, M., Greilinger, M., Schöner, W. & Blöschl, G. (2025) Increasing hourly heavy rainfall in Austria reflected in flood changes, *Nature*, **639**, 667–672. https://doi.org/10.1038/s41586-025-08647-2.

Hauser, M., Rauch, N., Gholami Korzani, M., Deletic, A. & Kleidorfer, M. (2025) Dynamic CA-ffé in Austria: fast flood modelling in alpine regions, *Proceedings of the 13th Urban Drainage Modelling Conference*. Innsbruck, Austria: University of Innsbruck.

Herzog, A. I. L. (2024) *Hydrodynamic sewer network calculation for the city of Innsbruck (in German: Hydrodynamische Kanalnetzberechnung der Stadt Innsbruck)*. Master thesis. University of Innsbruck, Innsbruck, Austria.

Hosseinzadehtalaei, P., Ishadi, N. K., Tabari, H. & Willems, P. (2021) Climate change impact assessment on pluvial flooding using a distribution-based bias correction of regional climate model simulations, *Journal of Hydrology*, **598**, 126239. https://doi.org/10.1016/j.jhydrol.2021.126239.

Huang, Y., Tian, Z., Ke, Q., Liu, J., Irannezhad, M., Fan, D., Hou, M. & Sun, L. (2020) Nature-based solutions for urban pluvial flood risk management, *WIRES Water*, **7**, e1421. https://doi.org/10.1002/wat2.1421.

Hussain, S. N., Zwain, H. M. & Nile, B. K. (2021) Modeling the effects of land-use and climate change on the performance of stormwater sewer system using SWMM simulation: case study, *Journal of Water and Climate Change*, **13**, 125–138. https://doi.org/10.2166/wcc.2021.180.

Hwang, J., Rhee, D. S. & Seo, Y. (2017) Implication of directly connected impervious areas to the mitigation of peak flows in urban catchments, *Water*, **9**, 696. https://doi.org/10.3390/w9090696.

IKB (2024) *Homepage of the sewer operator Innsbrucker Kommunalbetriebe (IKB)* [WWW Document]. https://www.ikb.at/30jahre/abwasser (accessed 10.14.25).

Jamali, B., Bach, P. M., Cunningham, L. & Deletic, A. (2019) A cellular automata fast flood evaluation (CA-ffé) model, *Water Resources Research*, **55**, 4936–4953. https://doi.org/10.1029/2018WR023679.

Khadka, A., Kokkonen, T., Niemi, T. J., Lähde, E., Sillanpää, N. & Koivusalo, H. (2020) Towards natural water cycle in urban areas: modelling stormwater management designs, *Urban Water Journal*, **17**, 587–597. https://doi.org/10.1080/1573062X.2019.1700285.

Kim, H., Jeong, H., Jeon, J. & Bae, S. (2016) The impact of impervious surface on water quality and its threshold in Korea, *Water*, **8**, 111. https://doi.org/10.3390/w8040111.

Kim, H., Kim, Y.-O. & Yang, S. (2025) Decoding urbanization effects on the water cycle: a multi-faceted analysis of balance, magnitude, and memory, *Hydrology Research*, **56**, 555–571. https://doi.org/10.2166/nh.2025.152.

Kleidorfer, M., Möderl, M., Sitzenfrei, R., Urich, C. & Rauch, W. (2009) A case independent approach on the impact of climate change effects on combined sewer system performance, *Water Science & Technology*, **60**, 1555–1564. https://doi.org/10.2166/wst.2009.520.

Kleidorfer, M., Sitzenfrei, R. & Rauch, W. (2014) Simplifying impact of urban development on sewer systems, *Water Science and Technology : A Journal of the International Association on Water Pollution Research*, **70**, 1808–1816. https://doi.org/10.2166/wst.2014.324.

Krvavica, N. & Rubinić, J. (2020) Evaluation of design storms and critical rainfall durations for flood prediction in partially urbanized catchments, *Water*, **12**(7), 2044. https://doi.org/10.3390/w12072044.

Kundzewicz, Z. W., Pińskwar, I. & Brakenridge, G. R. (2017) Changes in river flood hazard in Europe: a review, *Hydrology Research*, **49**, 294–302. https://doi.org/10.2166/nh.2017.016.

Laghari, A. N., Vanham, D. & Rauch, W. (2012) To what extent does climate change result in a shift in Alpine hydrology? A case study in the Austrian Alps, *Hydrological Sciences Journal*, **57**, 103–117. https://doi.org/10.1080/02626667.2011.637040.

Lenderink, G., de Vries, H., Fowler, H., Barbero, R., Ulft, B. & Meijgaard, E. (2021) Scaling and responses of extreme hourly precipitation in three climate experiments with a convection-permitting model, *Philosophical Transactions of The Royal Society A Mathematical Physical and Engineering Sciences*, **379** (2195): 2019054. https://doi.org/10.1098/rsta.2019.0544.

Liang, C., Zhang, X., Xia, J., Xu, J., She, D., Liang, C., Zhang, X., Xia, J., Xu, J. & She, D. (2020) The effect of sponge city construction for reducing directly connected impervious areas on hydrological responses at the urban catchment scale, *Water*, **12** (4), 1163. https://doi.org/10.3390/w12041163.

Liu, W., Chen, W. & Peng, C. (2014) Assessing the effectiveness of green infrastructures on urban flooding reduction: a community scale study, *Ecological Modelling*, **291**, 6–14. https://doi.org/10.1016/j.ecolmodel.2014.07.012.

Mikovits, C., Tscheikner-Gratl, F., Jasper-Tönnies, A., Einfalt, T., Huttenlau, M., Schöpf, M., Kinzel, H., Rauch, W. & Kleidorfer, M. (2017) Decision support for adaptation planning of urban drainage systems, *Journal of Water Resources Planning and Management*, **143** (12), 04017069. https://doi.org/10.1061/(ASCE)WR.1943-5452.0000840.

Miller, J. D. & Hutchins, M. (2017) The impacts of urbanisation and climate change on urban flooding and urban water quality: a review of the evidence concerning the United Kingdom, *Journal of Hydrology: Regional Studies*, **12**, 345–362. https://doi.org/10.1016/j.ejrh.2017.06.006.

Moon, H.-T., Kim, J.-S., Chen, J., Yoon, S.-K. & Moon, Y.-I. (2024) Mitigating urban flood Hazards: hybrid strategy of structural measures, *International Journal of Disaster Risk Reduction*, **108**, 104542. https://doi.org/10.1016/j.ijdrr.2024.104542.

Mugume, S. N., Kibibi, H., Sorensen, J. & Butler, D. (2024) Can blue-Green infrastructure enhance resilience in urban drainage systems during failure conditions?, *Water Science & Technology*, **89**, 915–944. https://doi.org/10.2166/wst.2024.032.

Municipal agency NRW (2016) Guideline for municipal heavy rain risk management in Baden-Württemberg (in German: Leitfaden Kommunales Starkregenrisikomanagement in Baden-Württemberg) [WWW Document]. https://pudi.lubw.de/detailseite/-/publication/47871.

Nie, L., Lindholm, O., Lindholm, G. & Syversen, E. (2009) Impacts of climate change on urban drainage systems – a case study in Fredrikstad, Norway, *Urban Water Journal*, **6**, 323–332. https://doi.org/10.1080/15730620802600924.

ÖWAV-RB 11 (2009) *Guideline for Wastewater Engineering Calculation and Dimensioning of Sewers; 2nd Completely Revised Edition*. Vienna: Austrian Standards Institute.

ÖWAV-RB45 (2015) *Guideline for Surface Drainage by Infiltration Into the Subsoil*. Vienna: Austrian Standards Institute.

Pfahl, S., O'Gorman, P. A. & Fischer, E. M. (2017) Understanding the regional pattern of projected future changes in extreme precipitation, *Nature Climate Change*, **7**, 423–427. https://doi.org/10.1038/nclimate3287.

Rosenzweig, B. R., McPhillips, L., Chang, H., Cheng, C., Welty, C., Matsler, M., Iwaniec, D. & Davidson, C. I. (2018) Pluvial flood risk and opportunities for resilience, *WIRES Water*, **5**, e1302. https://doi.org/10.1002/wat2.1302.

Rossman, L. A. (2015) *Storm Water Management Model User's Manual Version 5.1 [WWW Document]*. Washington, DC: Environmental Protection Agency. EPA/600/R-05/040, 2004. https://nepis.epa.gov/Exe/ZyPURL.cgi?Dockey=P100ERK4.txt.

Rybka, H., Haller, M., Brienen, S., Brauch, J., Früh, B., Junghänel, T., Lengfeld, K., Walter, A. & Winterrath, T. (2022) Convection-permitting climate simulations with COSMO-CLM for Germany: analysis of present and future daily and sub-daily extreme precipitation, *Meteorologische Zeitschrift*, **32**, 91–111. https://doi.org/10.1127/metz/2022/1147.

Sagar Kumar, M. & Umamahesh, N. V. (2025) Assessing low-impact development strategies using synthetic rainfall under climate change across different urbanization densities, *Water Science & Technology*, **91**, 1220–1233. https://doi.org/10.2166/wst.2025.070.

Wang, J., Zhang, S. & Guo, Y. (2019) Analyzing the impact of impervious area disconnection on urban runoff control using an analytical probabilistic model, *Water Resources Management*, **33** (5), 1753–1768. https://doi.org/10.1007/s11269-019-02211-0.

Wartalska, K., Kaźmierczak, B., Nowakowska, M. & Kotowski, A. (2020) Analysis of hyetographs for drainage system modeling, *Water*, **12**, 149. https://doi.org/10.3390/w12010149.

Wartalska, K., Szymczewski, S., Domalewska, W., Wdowikowski, M., Przestrzelska, K., Kotowski, A. & Kaźmierczak, B. (2025) The impact of climate change on the functioning of drainage systems in industrial areas – a case study, *Atmosphere*, **16**, 347. https://doi.org/10.3390/atmos16030347.

Wu, X. & Willems, P. (2025) Assessing blue-green infrastructures for urban flood and drought mitigation under changing climate scenarios, *Journal of Hydrology: Regional Studies*, **62**, 102798. https://doi.org/10.1016/j.ejrh.2025.102798.

Zhou, Q., Leng, G. & Huang, M. (2018) Impacts of future climate change on urban flood volumes in Hohhot in northern China: benefits of climate change mitigation and adaptations, *Hydrology and Earth System Sciences*, **22**, 305–316. https://doi.org/10.5194/hess-22-305-2018.

First received 7 November 2025; accepted in revised form 11 February 2026. Available online 27 February 2026